



UNIVERSITY OF LEEDS

This is a repository copy of *Permeability of fault rocks in siliciclastic reservoirs: Recent advances*.

White Rose Research Online URL for this paper:
<http://eprints.whiterose.ac.uk/125360/>

Version: Accepted Version

Article:

Fisher, QJ orcid.org/0000-0002-2881-7018, Haneef, J, Grattoni, CA
orcid.org/0000-0003-4418-2435 et al. (2 more authors) (2018) Permeability of fault rocks in siliciclastic reservoirs: Recent advances. *Marine and Petroleum Geology*, 91. pp. 29-42. ISSN 0264-8172

<https://doi.org/10.1016/j.marpetgeo.2017.12.019>

(c) 2017 Elsevier Ltd. Licensed under the Creative Commons Attribution-Non Commercial No Derivatives 4.0 International License
(<https://creativecommons.org/licenses/by-nc-nd/4.0/>).

Reuse

This article is distributed under the terms of the Creative Commons Attribution-NonCommercial-NoDerivs (CC BY-NC-ND) licence. This licence only allows you to download this work and share it with others as long as you credit the authors, but you can't change the article in any way or use it commercially. More information and the full terms of the licence here: <https://creativecommons.org/licenses/>

Takedown

If you consider content in White Rose Research Online to be in breach of UK law, please notify us by emailing eprints@whiterose.ac.uk including the URL of the record and the reason for the withdrawal request.

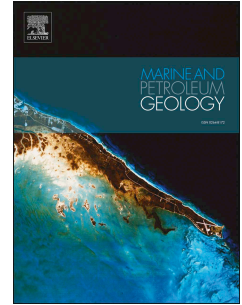


eprints@whiterose.ac.uk
<https://eprints.whiterose.ac.uk/>

Accepted Manuscript

Permeability of fault rocks in siliciclastic reservoirs: Recent advances

Quentin Fisher, Javed Haneef, Carlos Grattoni, Samuel Allshorn, Piroska Lorinczi



PII: S0264-8172(17)30500-7

DOI: [10.1016/j.marpetgeo.2017.12.019](https://doi.org/10.1016/j.marpetgeo.2017.12.019)

Reference: JMPG 3174

To appear in: *Marine and Petroleum Geology*

Received Date: 5 July 2017

Revised Date: 7 December 2017

Accepted Date: 11 December 2017

Please cite this article as: Fisher, Q., Haneef, J., Grattoni, C., Allshorn, S., Lorinczi, P., Permeability of fault rocks in siliciclastic reservoirs: Recent advances, *Marine and Petroleum Geology* (2018), doi: 10.1016/j.marpetgeo.2017.12.019.

This is a PDF file of an unedited manuscript that has been accepted for publication. As a service to our customers we are providing this early version of the manuscript. The manuscript will undergo copyediting, typesetting, and review of the resulting proof before it is published in its final form. Please note that during the production process errors may be discovered which could affect the content, and all legal disclaimers that apply to the journal pertain.

Permeability of fault rocks in siliciclastic reservoirs: recent advances

Quentin Fisher¹, Javed Haneef², Carlos Grattoni¹, Samuel Allshorn¹,
Piroska Lorinczi¹

¹ *School of Earth and Environment, University of Leeds, Leeds, UK*

² *NED University of Engineering & Technology, Karachi, Pakistan*

Abstract

It is common practice to create geologically realistic production simulation models of fault compartmentalized reservoirs. Data on fault rock properties are required, to calculate transmissibility multipliers that are incorporated into these models, to take into account the impact of fault rocks on fluid flow. Industry has generated large databases of fault rock permeability, which are commonly used for this purpose. Much of the permeability data were collected using two inappropriate laboratory practices with measurements being made at low confining pressure with distilled water as the permeant. New fault rock permeability measurements have been made at high confining pressures using formation compatible brines as the permeant. Fault permeability decreases by an average of five fold as net confining pressure is increased from that used in previous measurements (i.e. ~70 psi) to that approaching in situ conditions (i.e. 5000 psi). On the other hand, permeability increases by around the same amount if reservoir brine is used as the permeant instead of distilled water. So overall, these two inappropriate laboratory practices used in previous studies cancel each other out meaning that legacy fault rock

property data may still have value for modelling cross-fault flow in petroleum reservoirs.

A poor correlation exists between clay content and fault rock permeability, which is easily explained by the application of a simple clay-sand mixing model. This emphasises the need to gather fault permeability data directly from the reservoir of interest. The cost of such studies could be significantly reduced by screening core samples using a CT scanner so that only samples that are likely to impact fluid flow are analyzed in detail. The stress dependence of fault permeability identified in this study is likely to be primarily caused by damage generated during or following coring. So it is probably not necessary to take into account the impact of stress on fault permeability in simulation models unless the faults of interest are likely to reach failure and reactivate.

Keywords: fault rock, permeability, fault seal analysis, shale gouge ratio

1 Introduction

Faults are one of the main causes of reservoir compartmentalization. Understanding their impact on fluid flow is important for predicting reservoir performance and planning development strategies. For example, unexpected fault-related compartmentalization can lead to dramatic reserve write-downs or even project abandonment. On the other hand, unswept compartments are potentially profitable targets for infill drilling. Well-established workflows now exist for creating production simulation models that treat faults in a geologically-realistic manner (Fisher and

Jolley, 2007). Faults may act as total barriers or baffles to fluid flow in two distinct ways. Firstly, they juxtapose reservoir against non-reservoir rock creating what are known as juxtaposition seals, which generally act as very effective barriers to fluid flow. Secondly, fault gouge is often developed along faults, which itself may act as a barrier or baffle to fluid flow. Accurately modelling juxtaposition seals requires detailed knowledge of the sedimentary and structural architecture of the reservoir, which is obtained by integrating seismic, wire-line log and core data. The presence of fault gouge is generally modelled by including transmissibility multipliers in simulation models that require the permeability and thickness of fault rocks as well as information on the permeability of the undeformed reservoir and the dimensions of gridblocks within the simulation model (Manzocchi et al., 1999). More sophisticated analysis is occasionally conducted that takes into account the multiphase flow properties of fault rocks such as the capillary pressure and relative permeability (Manzocchi et al., 2002; Al-Busafi et al., 2005; Zijlstra et al., 2007; Al-Hinai et al., 2008; Tückmantel et al., 2012). A range of software tools exist to implement these workflows. These range from modules or plugins to standard geological modelling tools such as PetrelTM and RMSTM to sophisticated standalone tools such as TransgenTM. The latter is the only tool available that provides a robust methodology to incorporate the two phase flow properties of faults into simulation models.

High quality data on fault rock properties are central to the success of creating geologically-realistic simulation models of fault compartmentalized reservoirs. Industry has therefore made a significant investment in generating databases of the properties of fault rocks obtained from core retrieved from petroleum reservoirs (Fisher and Knipe, 1998, 2001; Frischbutter et al., 2017). The main contents of such

databases are an indication of the type of fault rock present, the clay content of the protolith, as well as the permeability of the fault rock and its protolith.

Unfortunately, there exist several significant uncertainties about the quality of the fault permeability data. In particular, industry has made a concerted effort to measure properties of fault rocks found within cores taken from petroleum reservoirs. This is sensible because it means that it is possible to populate simulation models with properties that are measured directly on the reservoir of interest (Jolley et al., 2007). Unfortunately, it has often proven difficult to obtain core plugs containing fault rocks from cores for two reasons. Firstly, faults are often not ideally orientated to take standard 1 or 1.5 in core plugs in the core sections that are made available for sampling. Secondly, even when faults are optimally orientated to allow plugs to be drilled there is a high incidence of failure due to the core plugs breaking along the faults. To get around these issues a workflow was developed in which small rectilinear blocks containing fault rock were cut from these cores (Fisher and Knipe, 1998, 2007). These were then placed in cylindrical molds and set in resin so that they could be loaded into core holders for permeability analysis. The soft nature of the resin used meant that analysis could only be conducted at confining pressures of less than 1 MPa (e.g. Fisher and Knipe, 1998, 2001). It is, however, well known that laboratory measurements of the permeability of tight rocks are very stress sensitive (Thomas and Ward, 1972; Wei et al., 1986; Kilmer et al., 1987; Morrow et al., 1984). For example, routine core analysis permeability measurements on 0.001mD tight gas sandstones may be over two orders of magnitude higher than for measurements made at in situ stress conditions (**Figure 1**). If this is also the case for fault rocks, the most commonly used workflow for incorporating fault rock properties into simulations

models could be based on measurements that overestimate fault permeability by several orders of magnitude.

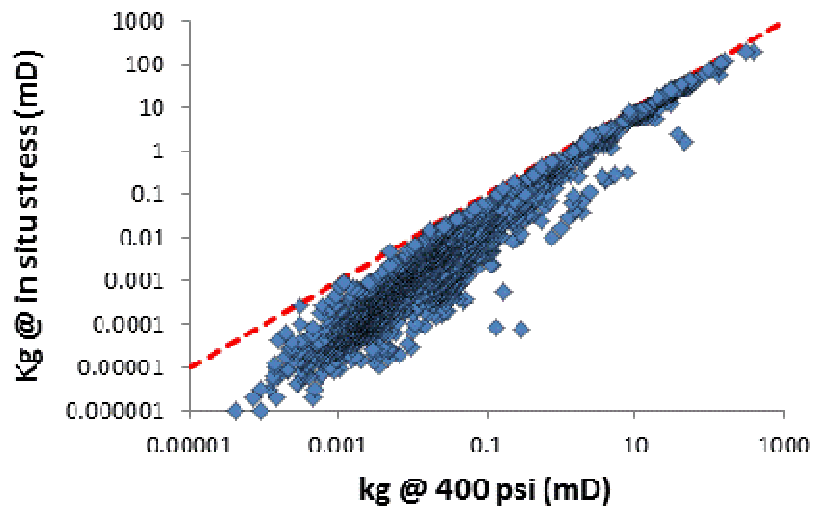


Figure 1 Plot of routine core analysis vs in situ permeability for tight gas sandstones (based on Byrnes and Castle, 2000). The original RCA data have been Klinkenberg corrected to highlight stress dependence of permeability. The red line is a 1:1 correlation.

A second problem was that there was a reluctance to use formation compatible brines during permeability measurements because they tended to corrode the pumps used to control flow through the samples during analysis. Consequently, many tests were performed using distilled water as the permeant. It is, however, well known that laboratory measurements of the permeability can be very sensitive to the brine composition, especially when clays are present (Lever and Dawe, 1987). For example, replacing a 3% NaCl brine with 1% NaCl may reduce the permeability of clay bearing sandstone by almost two orders of magnitude (**Figure 2**). If this is also the case for fault rocks, the most commonly used workflow for incorporating fault rock properties into simulations models could be based on measurements that are incorrect.

The aim of this paper is to address these two issues by presenting new data on the single phase flow properties of fault rocks. It should be noted that there are many published studies where high quality permeability measurements have been made on samples obtained from outcrops (e.g. Wibberley and Shimamoto, 2003; Al-Hinai et al., 2008; Sallet and Wibberley, 2013). However, such measurements are often not used directly by industry as input for flow simulations because of the preference to use data obtained directly from the reservoir of interest. The current study therefore focuses on measurements made on faults found within core material retrieved from petroleum reservoirs. The paper concentrates on the impact on different experimental protocols on the results of fault permeability analysis. Unfortunately, the dataset presented isn't sufficiently large to investigate key controls on fault permeability such as fault throw, timing of faulting and time-temperature history but is sufficiently large to assess the impact of clay content on fault permeability. The remainder of this paper begins by describing the samples analyzed and the experimental methods used in the study. The results are then presented and their implications are discussed. Finally, conclusions from the study are presented.

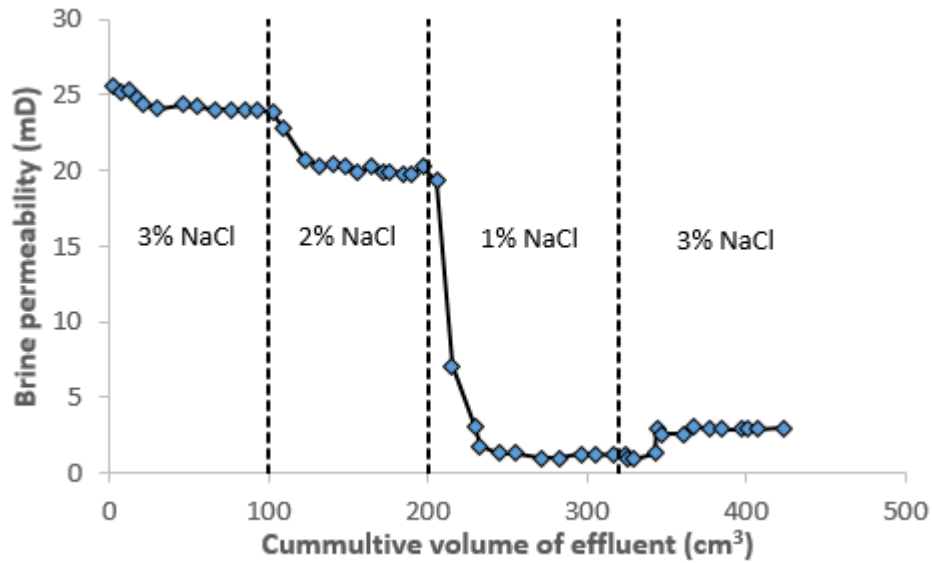


Figure 2 Water-sensitivity of the Spiney sandstone, Moray Firth Basin. Note the large decrease in permeability when the brine is changed to 1% NaCl (based on Lever and Dawe, 1987).

2 Methods

2.1 Samples studied

The study aims to assess the impact of using two inappropriate laboratory practices (low stress and distilled water) to analyse fault permeability. It is likely that much of the stress sensitivity of the permeability of tight rocks is a result of damage created during and following coring. So it was necessary to work on core material to understand the impact of previous inappropriate laboratory practices on fault permeabilities. Outcrop samples are also included for comparative purposes.

Around 50 fault rock samples from core and 35 fault rock samples from outcrop were examined; the locations and age of the samples are provided in **Table 1**. The study purposefully avoided analysing disaggregation zones and clay smears because the

former have been shown not to impact on fluid flow whereas the latter are likely to act as total barriers (Fisher and Knipe, 2001). Instead, the study has concentrated on cataclastic faults and phyllosilicate-framework fault rocks, which are more likely to act as baffles to flow in petroleum reservoirs. The samples chosen come from a wide range of sedimentary environments and have a wide range of burial histories and fault offsets. For example, samples from core tend to have small throws (0.1 to 1 cm) rarely with throws reaching >1 m. Fault rocks from outcrop have a far wider range of throws (<0.1 cm to ~70 m). Maximum burial depths vary from <0.5 km to 8 km and temperatures from ~50°C to 140°C.

Area	Outcrop/Core	Age	Number of samples
Norwegian Continental Shelf	Core	Jurassic	12
UK Central Graben	Core	Triassic & Jurassic	29
Offshore Netherlands	Core	Triassic	5
Gulf of Mexico	Core	Miocene	6
90 Fathom Fault	Outcrop	Permian	10
Vale of Eden, UK	Outcrop	Permian	7
Hopeman Fault, UK	Outcrop	Permian	5
Orange, France	Outcrop	Cretaceous	11

Airport Road exposure, Miri, Malaysia	Outcrop	Miocene	2
--	---------	---------	---

Table 1 Fault rock samples analysed during this study.

2.2 Sampling

The main aim of the study is to collect permeability data from fault rocks under high confining pressures and compare them with measurements using the same experimental methods used in previous studies. Core plugs are required to make permeability measurements at high confining pressure. In many cases, too little core was available to drill standard 1 or 1.5 inch core plugs. In such cases, smaller diameter (i.e. 16 and 20 mm diameter) core plugs were taken; these samples were then analysed in core holders specifically built to analyse these smaller diameter core plugs. Core plugs were drilled perpendicular to the fault so that fluid was forced to flow through the fault rock during permeability analysis. Blocks of $\sim 1.5 \text{ cm}^3$ size of the fault and undeformed sediment were also taken so that their permeability could be measured in a similar manner to most previous fault rock studies (i.e. Fisher and Knipe, 1998, 2001). Finally, blocks of 0.5 x 2 x 2 cm size were cut for SEM analysis. The overall sampling strategy is shown in **Figure 3**.

In all cases, the location from where samples were taken was guided by the CT scans. If the cores appeared poorly consolidated the core plugs were drilled frozen using diesel as the drilling fluid. The rectilinear blocks for petrophysical property analysis and SEM were cut using a thin diamond blade with diesel as the lubricant.

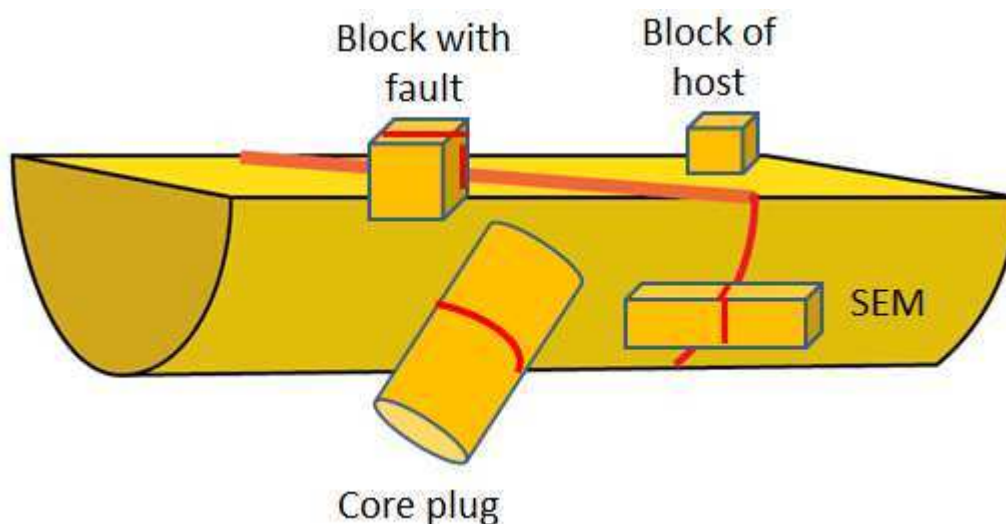


Figure 3 Diagram highlighting how the cores are sub-sectioned to obtain samples for microstructural and petrophysical property analysis.

2.3 Cleaning

Samples are thoroughly cleaned using Soxhlet extractor using a 50:50 mixture methanol-toluene/dichloromethane to remove any hydrocarbons and salts present. The samples were then dried in a humidity controlled oven at 60 °C for one week.

2.4 CT scanning

The internal structure of all core plugs was determined using a General Electrics, Brivo CT385. The CT images record differences in the degree of attenuation of the X-rays, which is material and energy dependent. The resolution of the scanner is around 0.25 mm but varies depending on factors such as the extent of beam hardening, positioning errors etc. The key aims of collecting these data were:-

- Identification of core damage prior to specimen analysis.
- Identification of sedimentary, structural and diagenetic heterogeneities.

In general, CT slices were taken at 1 cm intervals through the entire core sections provided.

2.5 Quantitative X-ray diffraction (QXRD)

QXRD data was obtained using the spray dry technique described by Hillier (1999; 2000). The sample was ground with 20 wt. % corundum, which acted as a standard. The slurry was then sprayed into a tube furnace using an air brush resulting in the formation of ~30 μm wide spherical aggregates with random mineral orientation. The spheres are then loaded into a sample holder and analysed using a Philips PW1050 XRD. The diffraction patterns obtained were analysed using the reference intensity ratio to calculate mineral abundances that are accurate to $\pm X^{0.35}$, where X is the mineral concentration in wt. %.

2.6 Microstructural analysis

Polished thin sections were carbon coated and then examined using a FEI Quanta 650 FEG SEM fitted with an Oxford Instruments INCA 350 EDX system/80mm X-Max SDD detector. The SEM was used to confirm the mineralogy determined by QXRD and to determine the diagenetic history of each sample. The fault rock was examined to determine the main deformation mechanisms, the processes responsible for altering the pore structure as well as the timing of faulting relative to the key diagenetic processes that affected the sample.

2.7 Absolute permeability analysis

A range of techniques was used for measuring the absolute permeability of rocks. In particular:

- Steady-state gas, Klinkenberg corrected, permeametry

- Steady-state liquid permeametry
- Pulse-decay gas permeametry
- Pulse-decay brine permeametry

In general, the pulse-decay technique is used to analyze samples with a permeability of <0.1 mD. The steady-state technique is used to analyze samples with a permeability of >0.1 mD. Measurements on the rectilinear blocks were made at confining pressures of ~70 psig. Measurements on the core plugs were at net confining pressures of 500, 1500, 2000, 2500, 3000, 4000 and 5000 psig.

2.7.1 Gas permeability

2.7.1.1 Klinkenberg corrected steady-state gas permeability analysis

Steady-state gas permeametry was conducted using a purpose-built flow system to which a wide range of core holders can be used (Hasler, hydrostatic, triaxial). The core holders can operate at confining pressures of up to 10,000 psi. Flow of nitrogen gas was initiated through the sample by opening a valve separating the gas cylinder from the flowline to the upstream of the core holder. The flow rate, absolute pressure at the upstream and differential pressure between the upstream and downstream of the sample was monitored until steady-state flow was reached. The flow rates and pressure differentials were used to calculate permeability using the adaptation of Darcy's law that accounted for the gas compressibility:

$$k_g = \frac{2\mu LQ}{A(P_1^2 - P_2^2)} \quad (1)$$

where μ is the gas viscosity, L is the sample length, Q is the flow rate at ambient conditions, A is the cross sectional area of the sample and P_1 and P_2 are the pressures at the upstream and downstream side of the sample respectively.

An additional consequence of using gas for measuring permeability is that gas slip on the pore walls creates a deviation from the continuum flow, known as the Klinkenberg effect. Gas slippage results in a decrease in the measured gas permeability as the mean gas pressure increases. To correct for gas slippage, the permeability is determined at different mean gas pressures and the permeability extrapolated to infinite pressure to obtain the Klinkenberg corrected permeability (Donaldson and Tiab, 2004).

2.7.1.2 Pulse decay gas permeametry

The permeability of tight samples (<0.1 mD) was analysed using an adapted CoreLab 200 PDP pulse-decay permeameter similar to that described by Jones (1997). The 200 PDP can accurately measure gas permeabilities of 0.1 mD to 10 nD. The equipment was originally supplied with core holders for 1 in and 1.5 in cores to operate at confining pressures of up to 2500 psi. However, the system has been up-graded so that it can be used with a wide range of core holders (e.g. Hassler and triaxial) that can operate up to 10,000 psi confining pressures and gas pressures of up to 8,000 psi. The instrument is housed within a temperature controlled laboratory (± 0.5 °C over 24 hours), which allows us to measure effective permeabilities of <1 nD.

The sample is loaded into a core holder and a confining pressure is then applied. Upstream and downstream reservoirs as well as the sample are then filled helium to a pressure typically of ~1000 psig. Care is taken to ensure that pressure and thermal equilibrium is achieved throughout the sample. The valve separating the upstream volume, V_1 , from the core holder is then closed and the pressure in V_1 is increased by 2 - 3%. Once pressure in V_1 becomes stable the valve separating the

core holder from V_1 is opened and the differential and downstream pressures are monitored until pressure equilibrium has been achieved. Permeability is then calculated automatically from the pressure transient data by an on-line computer using the method outlined in Jones (1997). The measurement requires information on the pore volume of the sample, which is determined from a combination of Hg-immersion and He pycnometry.

2.7.2 Brine permeability

Samples were saturated with a brine with the same composition as the formation water, which varied depending upon where the samples were obtained. Outcrop samples were analysed with a 200,000 ppm brine and those with permeabilities of >0.1 mD were analysed using a steady-state method whereas those with lower permeability were measured using a pulse-decay system.

2.7.2.1 Steady state brine permeametry

Steady-state hydraulic conductivity tests are conducted using a permeameter based on the design of Olson & Daniel (1981) and Olson et al., (2001). The permeameter uses accurate constant-rate-of-flow pumps to control flow rates in and out of the core holder. The highly linear differential pressure transducers allow permeabilities from 10 D down to 0.001mD to be measured. In the current study, the instrument was only used to measure flow in samples with a permeability of >0.1 mD. Measurements were made in a core holder at could operate at confining pressures of up to 10,000 psi.

The permeability of the sample is determined using Darcy's law:

$$k = \frac{\mu L Q}{A(P_1 - P_2)} \quad (2)$$

where μ is the viscosity of the fluid, L is the sample length, Q is the volumetric flow rate, A is the cross sectional area of the sample and P_1 and P_2 are the upstream and downstream pressures.

2.7.2.2 Pulse-decay brine permeability

A purpose-built system based on Amaefule et al. (1986) was used to analyse samples with a permeability of <0.1 mD. The experimental arrangement consists of a cylindrical sample mounted in a high pressure core holder, up to 5000 psi for 16 to 25 mm diameter samples and 10000 psi for 38 mm diameter core plugs. The sample is connected upstream with a high pressure pump (Isco 100 DX) and downstream to a large liquid reservoir, which for practical purposes is infinite with respect to the upstream volume. The system is pressurized to the base pressure before starting the experiment to dissolve any air that may have been trapped in the system and allowed to equilibrate. The fluid pressure in the pump and upstream volume is increased at the start of the experiment, and suddenly connected to the upstream side of the sample. Liquid flows across the sample to the downstream reservoir as the pressure differential decays. The upstream pressure, temperature and differential pressures as a function of time are monitored and automatically recorded.

The permeability of the sample is first calculated using an approximated solution to evaluate the time needed for the late time exponential solution to be valid. The slope of $\ln(\Delta P)$ versus time is then used in the exponential solution to calculate the liquid permeability of the sample.

2.7.3 Calculation of fault rock permeability

In most cases, the core plugs or rectilinear blocks used for permeability analysis were not composed entirely of fault rock. Fault rock permeabilities therefore needed

to be deconvolved from the measurements by assuming that the permeability the sample containing the fault rock, k_{fs} is the length weighted harmonic average of the fault, k_f , and host rock, k_h , permeability so that:

$$k_f = \frac{L_f}{\frac{L_{fs}}{k_{fs}} - \frac{L_{fs} - L_f}{k_h}} \quad (3)$$

where L_f is the thickness of the fault rock within the sample being analysed and L_{fs} is the length of the sample containing the fault rock. L_{fs} is measured using a digital caliper whereas L_f is measured from CT scans of the samples being analysed.

3 Results

3.1 Microstructure and CT analysis

The sample classification scheme for fault rocks proposed by Fisher and Knipe (1998, 2001) has been used in this study. In particular, Fisher and Knipe (1998, 2001) suggested that fault rocks in siliciclastic sediments could be divided into:-

- **Disaggregation zones**, which are those which formed in clean sandstones that have not experienced significant grain fracturing.
- **Cataclastic faults** are those that form in clean sandstones and experience a significant reduction in porosity and permeability due to deformation-induced grain fracturing.
- **Phyllosilicate-framework fault rocks** develop from impure sandstones. Mixing of clays with framework grains resulted in a replacement of macroporosity with microporosity.
- **Clay smears** developed due to the deformation of clay-rich sediments.

Fisher and Knipe (1998, 2001) defined clean, impure and clay-rich sandstones as those with <14%, 14-40% and >40% clay respectively. In this study, the fault rocks have not been defined based on the clay content of the protolith but instead based on the microstructure of the fault rocks. Phyllosilicate-framework fault rocks were originally defined as developing from impure sandstones containing 15-40% clay/phyllosilicates (Knipe et al., 1998, 2001). Here phyllosilicate-framework fault rocks are defined as being grain-supported but with all space between the grains being filled by clays and microporosity. This slightly different definition was used to take into account the observation that the flow properties of fault rocks that have experienced cataclasis maybe controlled by a framework of intragranular phyllosilicates even when formed from sediments with clay contents of <15%. This is because cataclasis reduces grain sorting and intragranular porosity so less clay is needed to control the pore size distribution within the remained pore space. Clay smears are defined as being clay supported fault rocks. Disaggregation zones and cataclasites have pore space between the grains that is not dominated by their clay content. Such fault rocks have been divided according to the classification of Sibson (1977) in which disaggregation zones have a matrix composed of <10% fractured grains and cataclasites have a matrix of 50 to 90% fractured grains. Protocataclasite have been introduced to the classification of Fisher and Knipe (1998, 2001) to describe fault rocks composed of 10 to 50% fractured grains.

Overall, two samples classed as disaggregation zones, 10 protocataclasites, 57 cataclastic faults and 16 phyllosilicate-framework fault rocks where analysed during this study (**Table 2**). These are described separately below.

Fault rock type	Number
-----------------	--------

Disaggregation zones	2
Protocataclasites	10
Phyllosilicate-framework fault rock	16
Cataclastic faults	57
Clay smears	2

Table 2 Fault rock types present in the samples analysed during this study.

3.1.1 Disaggregation zones

Disaggregation zones are fault rocks formed in siliciclastic sandstones that experienced only small amounts of grain fracturing during faulting and whose macroporosity between grains is not filled by clay and microporosity. Disaggregation zones were purposefully avoided during this study as they do not have a significant impact on fluid flow. However, two were analysed. These are very subtle features in core and are very difficult to identify on CT scans (**Figure 4**). Microstructural analysis indicates that they have almost the same microstructure as their surrounding host sandstone (**Figure 5**).

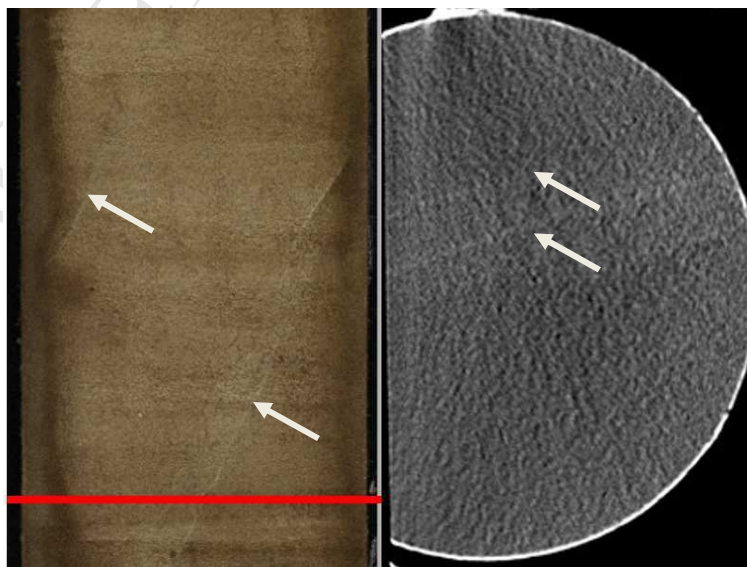


Figure 4 Left) Photograph of sample containing a disaggregation zone, and Right) CT scan through the sample; the position of the CT scan is marked by the red line in the photograph; the fault rock are marked by arrows.

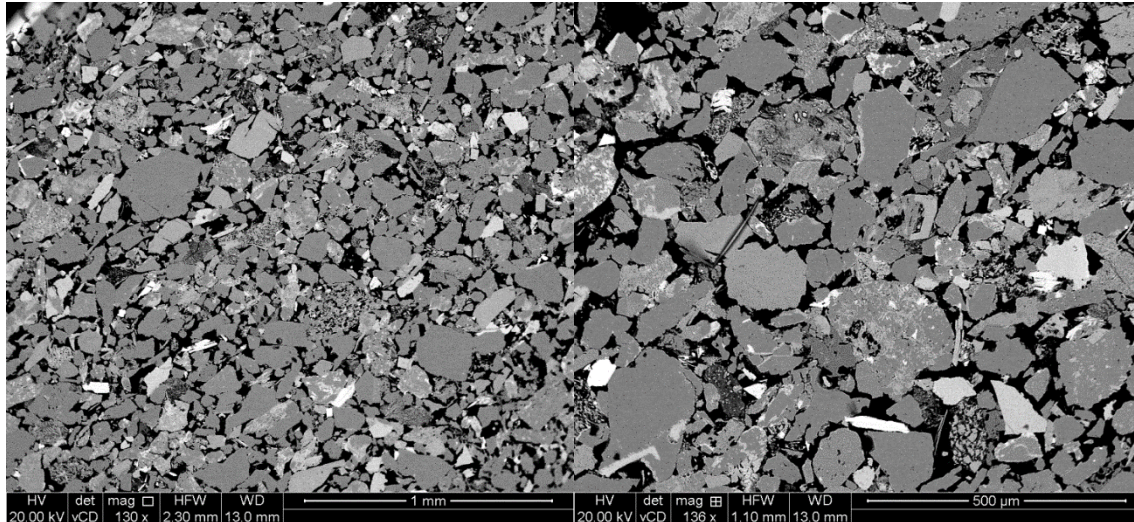


Figure 5 BSEM images showing: (Left) the host sandstone and (Right) the fault rock from the sample shown in **Figure 8**.

3.1.2 Protocataclastic faults

Protocataclastic faults are those that have a matrix composed of 10-50% grain fragments and the space between these grains is not dominated by clay and microporosity. Protocataclasites are far more obvious than disaggregation zones in both core photos and CT-scans (**Figure 6**). In particular, they tend to have a lighter colour than the host sandstone and CT-scans show them to be denser than their host sandstone. The increase in density is caused by deformation induced grain fracturing (**Figure 7**), which allows the grain fragments to be packed more efficiently than the undeformed sandstone. In addition, these fault rocks may experience enhanced post-deformation diagenesis, such as quartz cementation and enhanced grain-contact quartz dissolution, if they are buried beyond 90°C (Fisher and Knipe, 1998, 2001). Several protocataclastic fault rocks examined during this study contain

domains that have experienced enhanced grain-contact quartz dissolution. In all cases, these were in samples that contain small amounts of detrital mica that had been smeared along the fault and its presence at grain-contacts enhanced quartz dissolution.

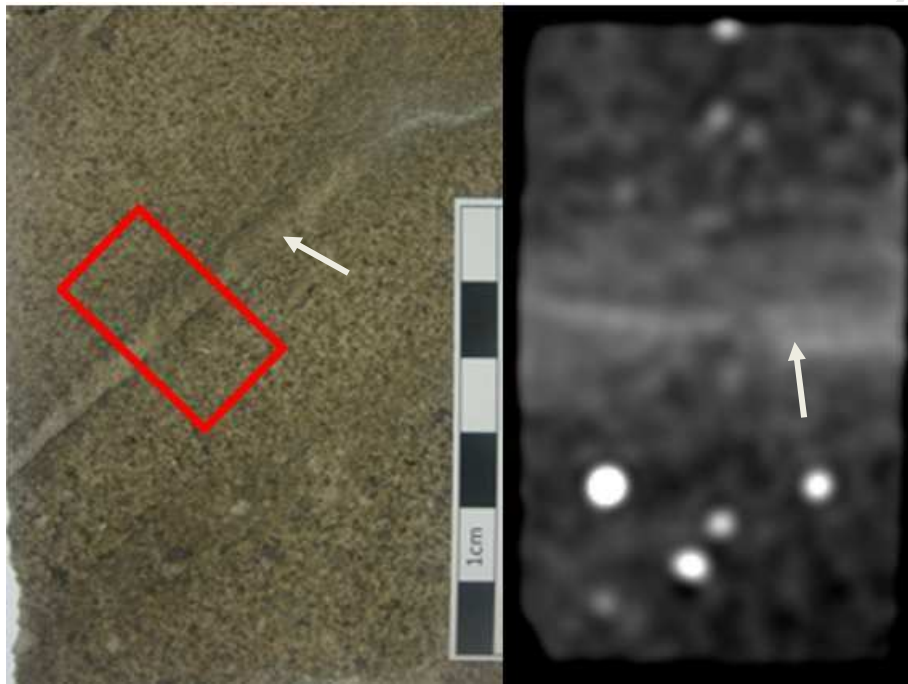


Figure 6 Left) Photograph of sample containing a protocataclastic fault, and Right) CT scan through the sample; the position of the CT scan is marked by the red rectangle in the photograph; the faults are marked by arrows.

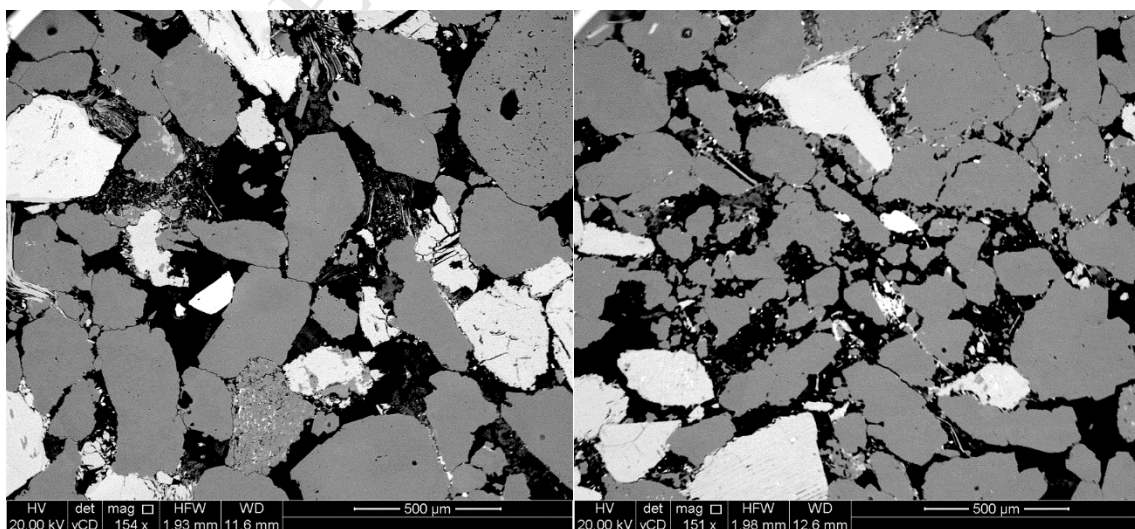


Figure 7 BSEM images showing: (Left) the host sandstone and (Right) the protocataclasite from the sample shown in **Figure 6**.

3.1.3 Cataclastic faults

Cataclastic faults are those that have a matrix composed of 50-90% grain fragments and the space between these grains is not dominated by clay and microporosity. Cataclastic faults are far more obvious in both core photos and CT-scans than both disaggregation zones and protocataclasites (**Figure 8**). In particular, they tend to have a lighter colour and CT-scans show them to be denser than their host sandstone. The increase in density is caused by deformation-induced grain fracturing (**Figure 9**), which allows the grain fragments to be packed more efficiently than the undeformed sandstone. These fault rocks may experience enhanced post-deformation diagenesis, such as quartz cementation and enhanced grain-contact quartz dissolution, if they are buried beyond 90°C. Several cataclastic fault rocks examined during this study experienced enhanced quartz cementation. It is likely that this reflects the increased reactive quartz surface area created by cataclastic deformation.

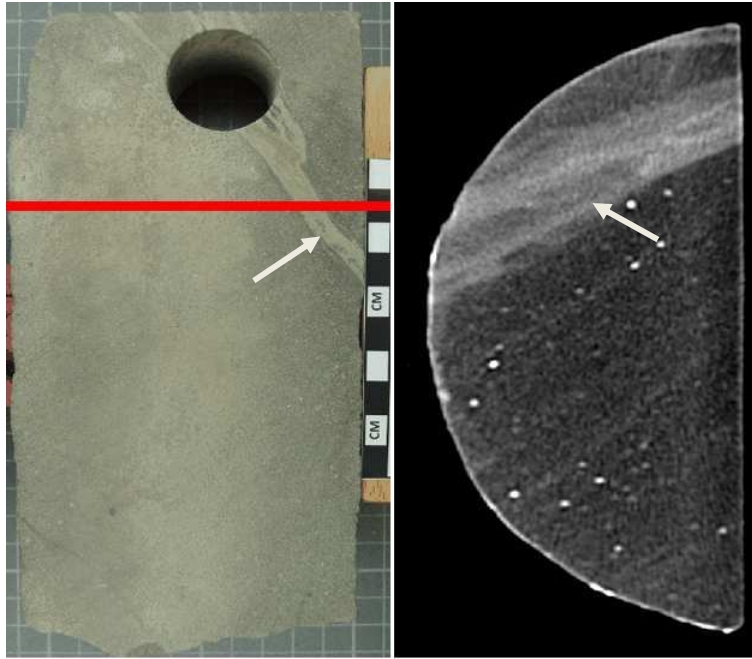


Figure 8 Left) Photograph of sample containing a cataclastic fault, and Right) CT scan through the sample; the position of the CT scan is marked by the red line in the photograph; the faults are marked by arrows.

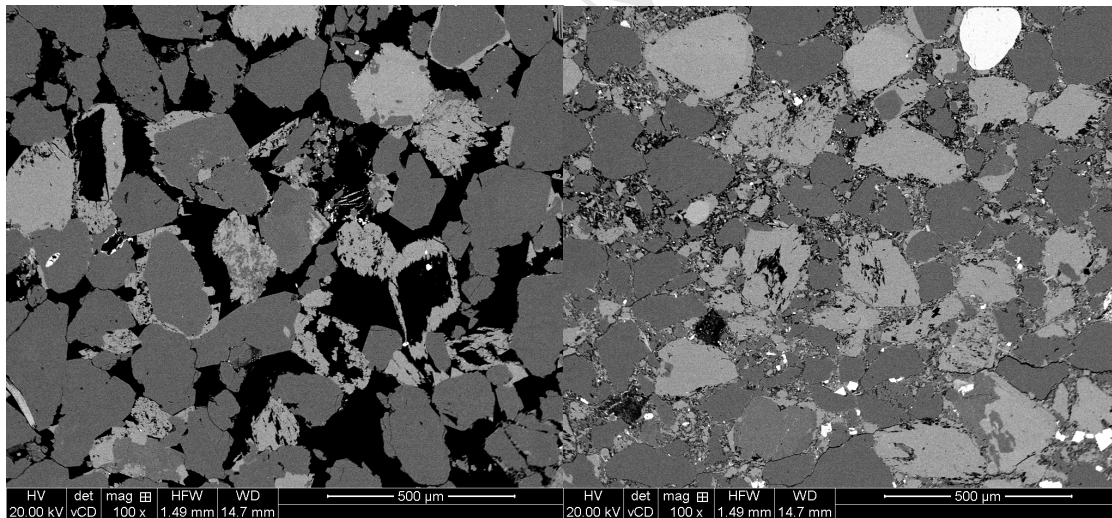


Figure 9 BSEM images showing: (Left) the host sandstone and (Right) the cataclastic fault rock from the sample shown in **Figure 8**.

3.1.4 Phyllosilicate-framework fault rocks

Phyllosilicate-framework fault rocks are grain-supported and the intragranular pore space between the grains is filled with clay and microporosity. Phyllosilicate-framework fault rocks often have a darker colour than their host sandstone and CT scans reveal that they are denser than their hosts (**Figure 10**). The increase in density is a result of two processes. First, clays become mixed with framework grains during faulting, which results in a replacement of macroporosity with clays and microporosity (**Figure 11**). Secondly, these fault rocks often experience enhanced grain-contact quartz deformation following faulting due to the deformation-induced incorporation at the contacts of quartz grains. In addition, phyllosilicate-framework fault rocks may experience grain fracturing during faulting.

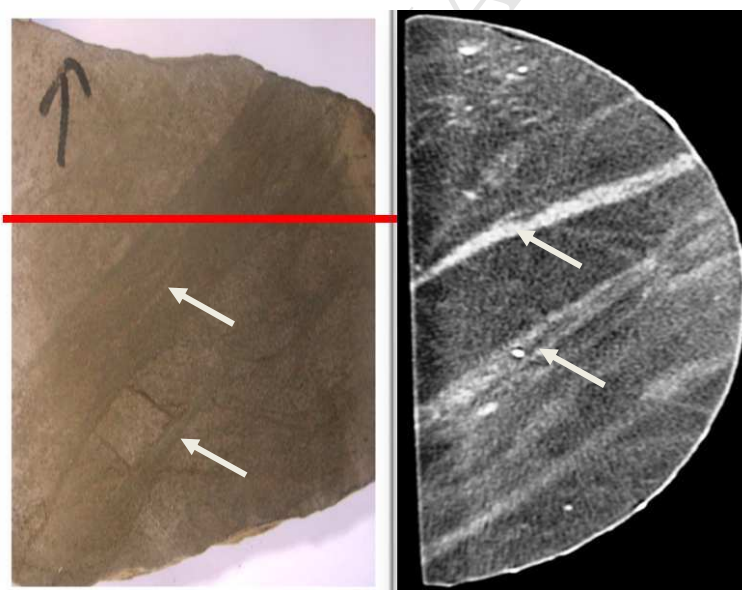


Figure 10 Left) Photograph of sample containing a phyllosilicate-framework fault rock, and Right) CT scan through the sample; the position of the CT scan is marked by the red line in the images and the faults are marked by arrows.

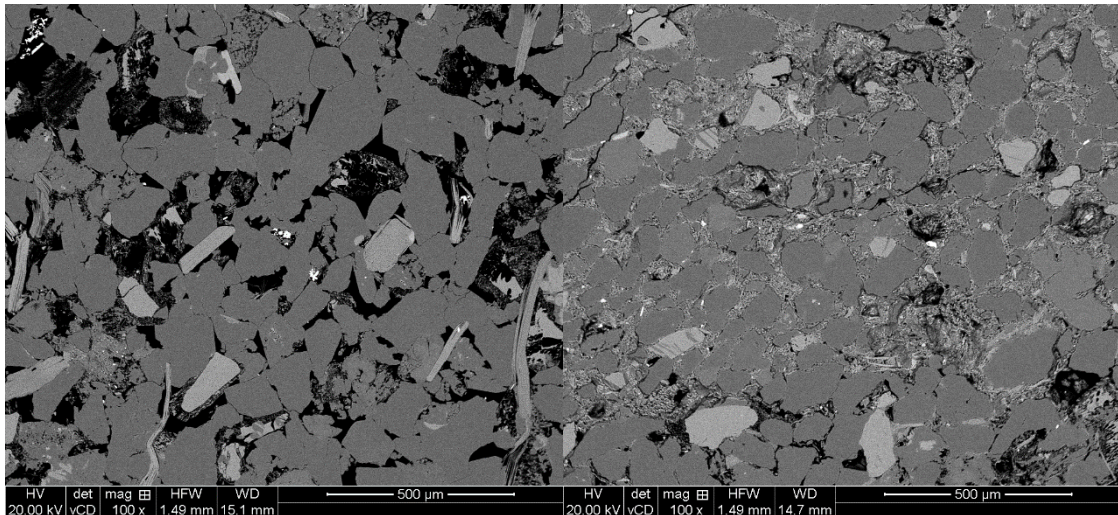


Figure 11 BSEM images showing: (Left) the host sandstone and (Right) the fault rock from the sample shown in **Figure 10**.

3.2 Stress dependency of permeability

The gas and brine permeabilities of the core plugs all decreased with increasing confining pressure (e.g. **Figure 12**). Increasing confining pressures from 500 psi to 5000 psi reduced permeability by around 50% (**Figure 13**) but decreases up to 90% are common. The stress dependency seems to be slightly lower than observed in a database of tight gas sandstones (**Figure 14**). The brine permeability of small number of samples decreases by over two orders of magnitude as net stress is increased from 500 to 5000 psi. Initially these samples were believed to be outliers, however, close examination shows that these fault rocks have a strong fabric created by enhanced grain-contact quartz dissolution (**Figure 15**). It is possible that the high aspect ratio grain boundaries are responsible for this high stress sensitivity.

There is a tendency for the stress dependence of permeability to increase with decreasing permeability. There is also a tendency of the permeability of samples from outcrop to be less stress dependent than those from core. The stress vs. fault

permeability data for each sample were fitted with a logarithmic relationship of the form:

$$k = A + B \ln(\sigma) \quad (4)$$

where k is permeability, A and B are fitting parameters and σ is the net confining pressure (i.e. total confining pressure minus pore pressure). This relationship was used to extrapolate the core plug data to the same confining pressure as the cubes containing the fault rock were analyzed so that the two sets of data could be compared.

There is approximately a 1:1 relationship between the permeabilities measured at ambient stress and those estimated by extrapolating the values obtained from the core plugs (**Figure 16**). A significant amount of scatter exists on these plots (i.e. >1 order of magnitude) but this is to be expected considering that: (i) faults are heterogeneous and the core plugs were taken next to where the rectilinear blocks for the ambient stress measurements were taken, and (ii) errors will always occur when extrapolating data outside the conditions at which they were measured. This large amount of scatter means that it is probably safer to compare the permeability extrapolated to low stress with the high stress measurements as an indication of the overall impact of making permeability measurements at ambient vs. in situ stress. The results indicate that the gas permeability of the fault rocks taken from core at in situ conditions averages around 20% that measured at ambient stress conditions (**Figure 17**). The fault rocks taken from outcrop appear slightly less stress sensitive with the values measured at 5000 psi net confining pressure being only 50% of the values measured at ambient stress.

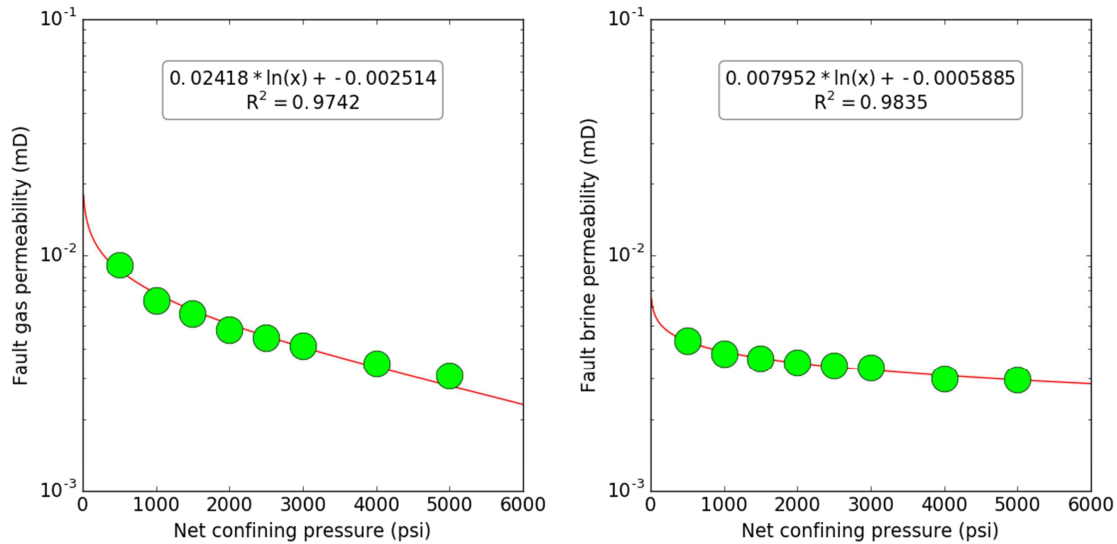


Figure 12 Examples of the stress dependence of: Left) gas and Right) brine permeabilities measured on core plug samples.

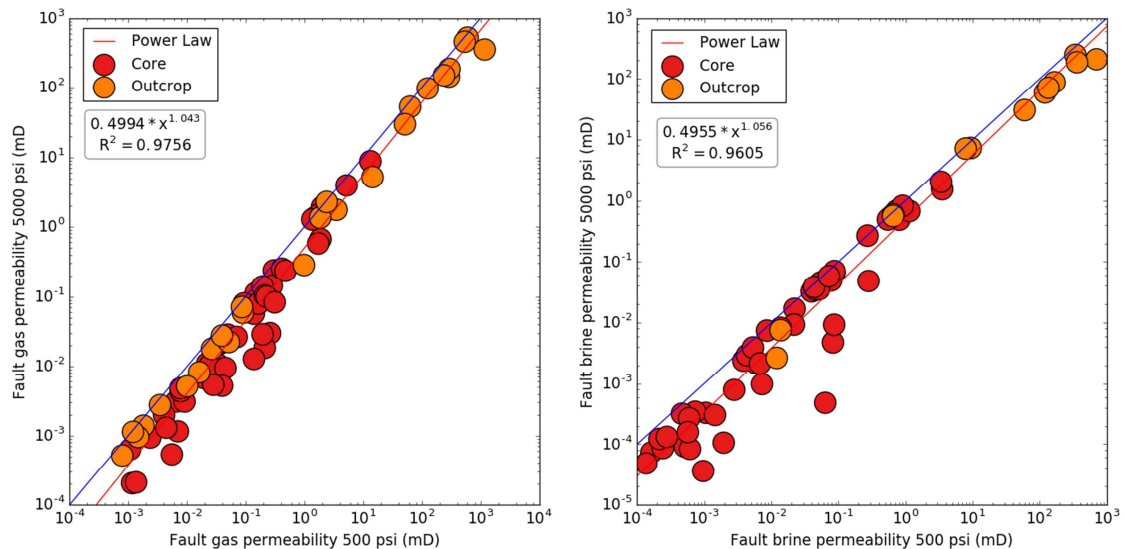


Figure 13 Plot of: Left) gas and Right) brine permeability of fault permeability measured at 500 psi net stress vs. the permeability measured at 5000 psi. A 1:1 line (blue) as well as a regression (red) are plotted. Points are coloured according to whether they were obtained from outcrop or core.

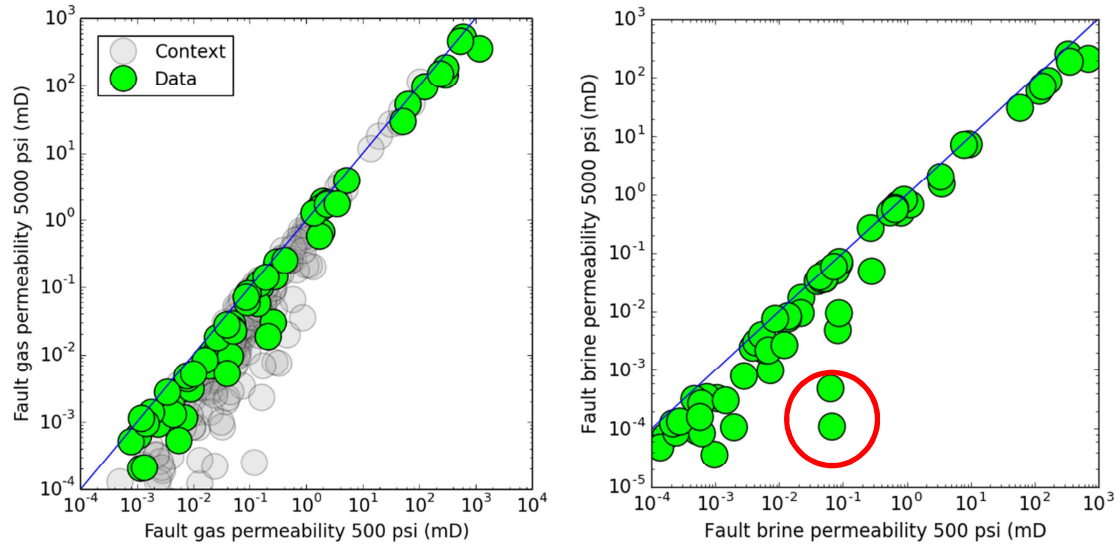


Figure 14 Plot of: Left) gas permeability measured at 500 psi confining pressure vs the value measured at 5000 psi - tight gas sandstone dataset (University of Leeds, unpublished) is presented as context; Right) brine permeability measured at 500 psi confining pressure vs. the value measured at 5000 psi - the outliers circled in red have experienced enhanced grain-contact quartz dissolution. The blue line is the 1:1 relationship between the plotted values.

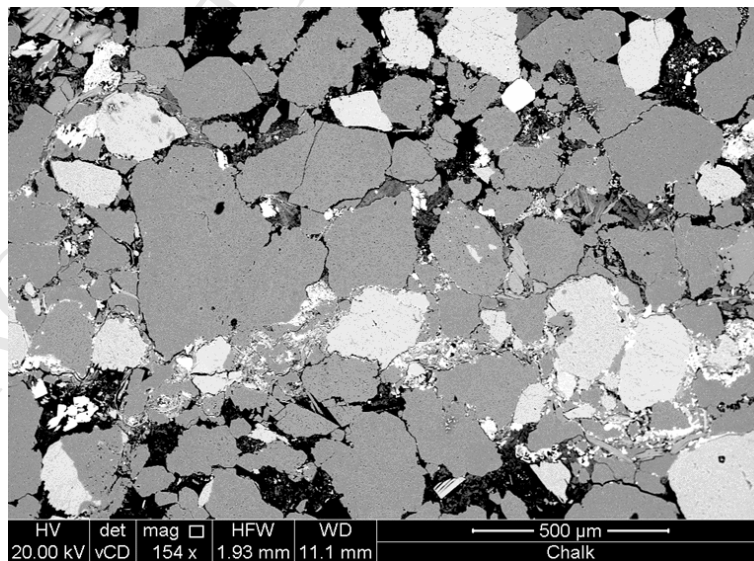


Figure 15 BSEM image showing the border of faults that have experienced enhanced grain-contact quartz dissolution; the brine permeability of these fault rocks appears particularly stress sensitive.

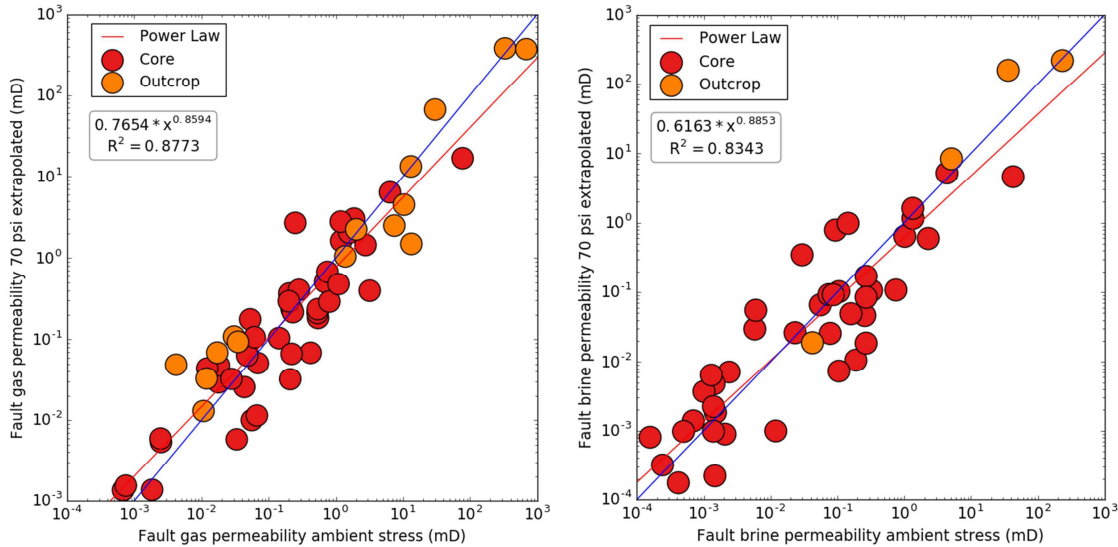


Figure 16 Plot of: Left) gas and Right) brine permeability measured at ambient stress against the value obtained by extrapolating the power-law relationship between stress and permeability to 70 psi, which is the same confining pressure at which the ambient stress measurements were made. A 1:1 line (blue) as well as a regression (red) are plotted. Points are coloured according to whether they were obtained from outcrop or core.

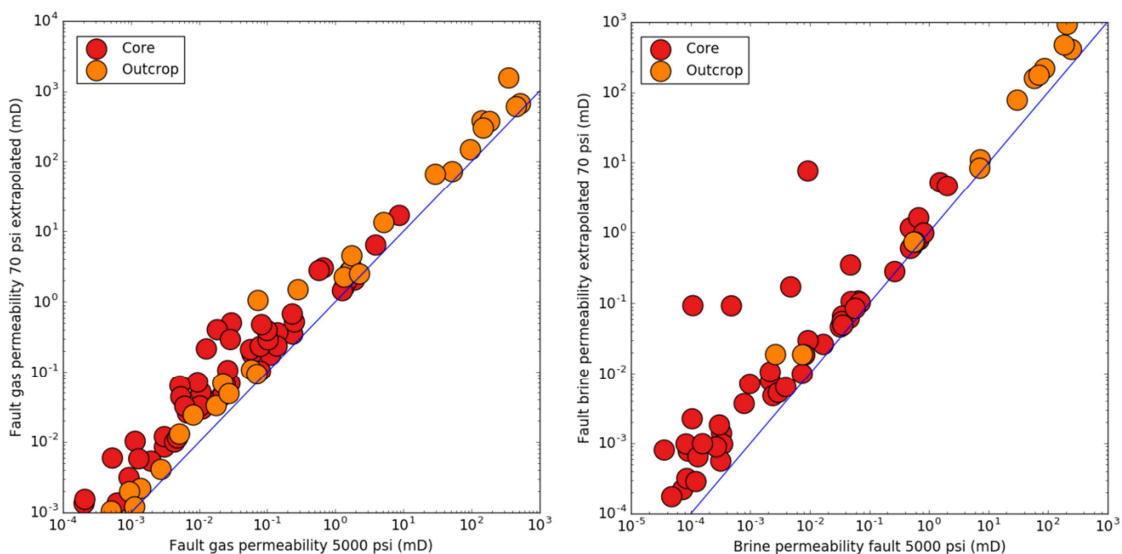


Figure 17 Plot of: Left) gas and Right) brine permeability measured at 5000 psi net confining pressure against the value obtained by extrapolating the power law relationship between stress and permeability to 70 psi, which is the same confining pressure at which the ambient stress measurements were made. A 1:1 line (blue) as well as a regression (red) are plotted. Points are coloured according to whether they were obtained from outcrop or core.

3.3 Impact of gas/fluid type on permeability

Gas vs brine permeability

The brine permeability of fault rock samples is around 25% that of the gas permeability irrespective of whether the measurements were made at ambient or high confining pressures (e.g. **Figure 18**). Overall, the relationship between gas and brine permeability is similar to tight gas sandstones. It does not appear that the difference between gas and brine permeability is significantly impacted by fault rock type or clay content.

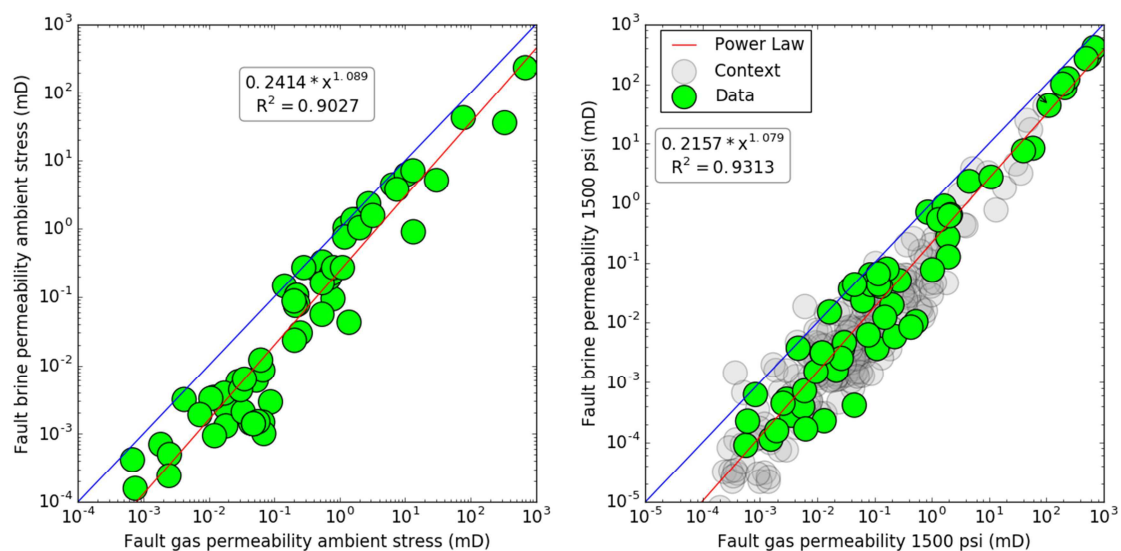


Figure 18 Plots of gas permeability vs brine permeability measured at Left) ambient stress and Right) 1500 psi confining pressure; a dataset collected for tight gas sandstones has

been included for comparison for the stressed measurements. The blue line represents the 1:1 relationship whereas the red line is the power-law regression.

Brine vs distilled water permeability

Permeability to brine and distilled water measured under ambient stress conditions showed that brine permeability is on average around 5 fold higher than permeability to distilled water (**Figure 19**). Overall, we expected that the difference between gas and brine permeability could be related to the clay content but we found this not to be the case. Rather surprisingly, the difference between brine and distilled water permeability appears to increase with increasing permeability. This provides an indication that a key control on the difference between brine and distilled water permeability could be related to the method used to make the measurements. In particular, the biggest differences between brine and distilled water permeability is higher in samples measured using the steady-state method compared to those measured using the pulse-decay method. One possible reason for this is that the higher flow rates in the steady-state test could result in the movement of fines and hence a blocking of pore throats.

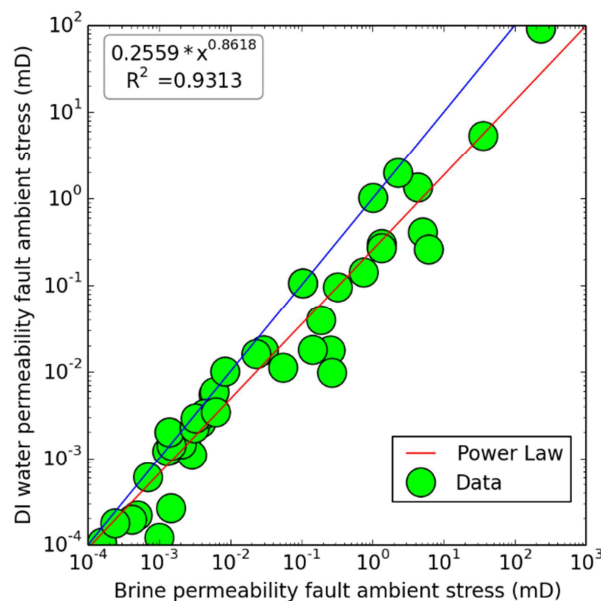


Figure 19 Plot of the distilled water against brine permeability for fault rocks measured at ambient stress. The blue line represents the 1:1 relationship whereas the red line is the power-law regression.

Clay vs fault rock permeability

The clay content of thin faults such as those that are found in core cannot be measured directly using QXRD. The small throw of the faults (generally <1 cm) mean that it often assumed that the clay content of the host sediment is similar to that of the fault rock. The data collected during the current study indicates that fault permeability is not strongly correlated with either clay content or fault rock type (Figure 20).

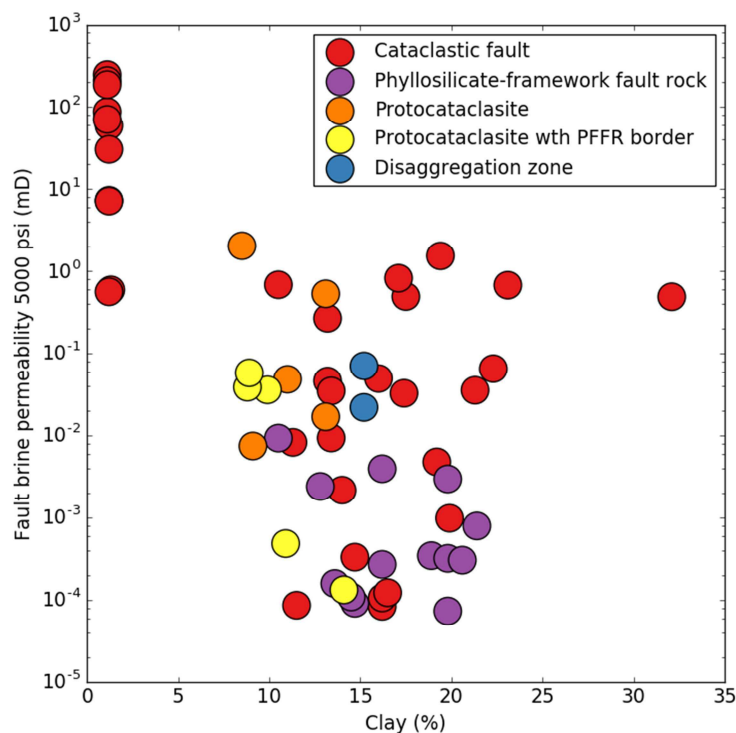


Figure 20 Plot of clay content vs brine permeability coloured according to fault rock type.

4 Discussion

4.1 Implications for legacy fault rock property data

The primary aim of this study was to assess the implications of using legacy fault rock property data being collected under inappropriate laboratory conditions in fault seal analyses. The results presented in this paper indicate that fault permeability under ambient stress averages four times that collected under in situ stress (**Figure 17**). On the other hand, the permeability measured using distilled water is around one fifth of that measured using a formation compatible brine (**Figure 19**). So overall, the effects of using distilled water on the cubes partly cancels out the effect of making measurements at low stresses. The permeability to distilled water at ambient stress is on average around the same as that measured using brine at in situ stress (**Figure 21**). This is an important result as it suggests that there remains some justification to continue use permeability values in many of the fault rock property databases used by companies. However, such data should only be used with the knowledge that the permeability of a specific fault rock sample measured at low stress and using formation incompatible brine could be in error by over an order of magnitude. It should also be emphasised that it is recommended that future fault rock permeability measurements are made at in situ stress conditions using formation compatible brine.

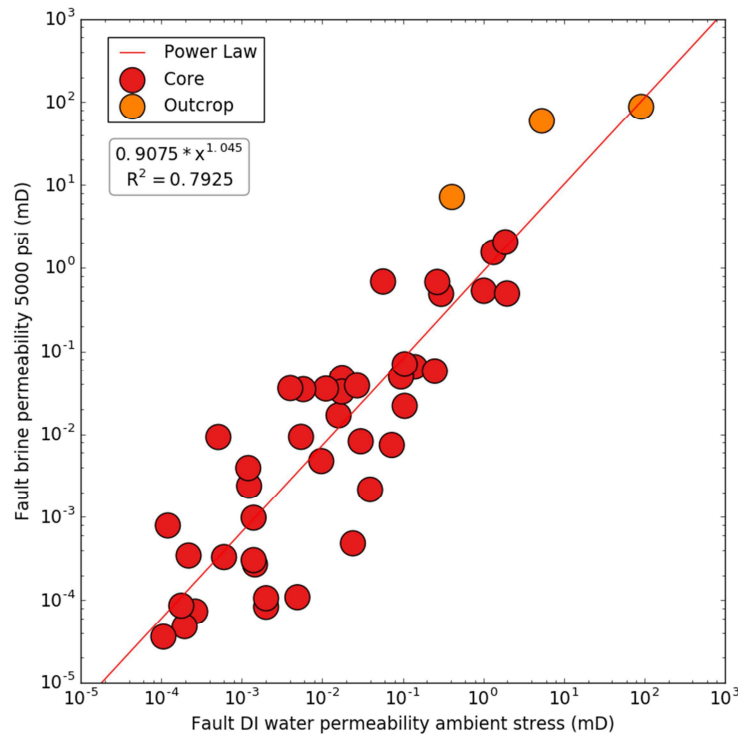


Figure 21 Plot of fault permeability measured using distilled water at ambient stress vs brine permeability at 5000 psi confining pressure. The red line represents the power-law regression; note that there is nearly a 1:1 correlation.

4.2 Causes of stress dependency

The permeability of fault rock samples analysed during the current study proved to be very stress dependant in laboratory experiments. If this were true in the subsurface, the fault properties incorporated into production simulation models would need to take into account variability as a function of changes in effective stress. Implementing a stress dependant fault transmissibility is relatively trivial in reservoirs where the change in effective stress at a particular position can be easily calculated from the change in fluid pressure. However, this is not the case in reservoirs that experience stress arching during production (Segura et al., 2011). In such reservoirs, fault properties might need to be updated based on the results of coupled flow-geomechanical models, which are time consuming and expensive to construct and

the technology is in its infancy compared to simulation models. It's therefore probably not worth making the effort to incorporate the stress dependency of fault permeability into production simulation based on the results from the current study unless it is likely that the faults are likely to reactivate as a result of production.

The fault rock samples examined during the current study have had permeabilities that are stress dependent but to varying degrees. Three key points emerge from the results:

- Outcrop samples seem less stress dependent
- The samples seem less dependent than tight gas sandstones
- Fault rocks are likely to experience higher effective stresses than those used in the experiments reported in this study.

An interpretation of these points is that the reason why the permeability of fault rocks are stress sensitive in the laboratory is due to damage created during and following coring. In particular, SEM analysis revealed the presence of microfractures at grain contacts that have a width of 0.5 to 3 μm (**Figure 22**). It is unlikely that these could remain open in petroleum reservoirs and instead are likely to have formed during or following coring. Indeed, micro-CT scans of tight gas sandstones have shown that these close when confining pressure is increased to in situ values (pers com. Prof. Mark Knackstedt, ANU). In addition, a recent study investigating the stress dependence of the capillary pressure injected molten Fields metal into several tight rocks at a low confining pressure and then conducted microstructural analysis on samples in which the Fields metal had been allowed to solidify at different confining pressures (Eardley, 2017). The results showed that flow at low confining pressures was dominated by microfracture arrays that closed when confining pressure was increased to in situ conditions. It seems likely that such features are the cause of the

stress dependency of fault permeability and so their absence in the subsurface would mean that the permeability of fault rocks would not be as stress sensitive as in the laboratory so long as differential stresses did not rise to the level needed to cause failure.

The reason why the permeability of some tight gas sandstone samples might be more stress sensitive than the fault rock samples could reflect the fact that the faults analysed during the current study were relatively thin (i.e. 1 to 0.5 mm). The thin nature of the fault rocks may have allowed fluid pressures to equilibrate more easily during core extraction than was the case for the tight gas sandstone cores, which tend to have uniformly low permeability.

Overall, these results may simplify the modelling cross-fault flow because it means that in reservoirs in which chemical compaction has taken over from mechanical compaction as the main porosity-reduction mechanism there is little need to take into account the stress sensitivity of fault rock permeability, which will simplify modelling considerably, unless it is likely that the faults are likely to reactivate as a result of production.

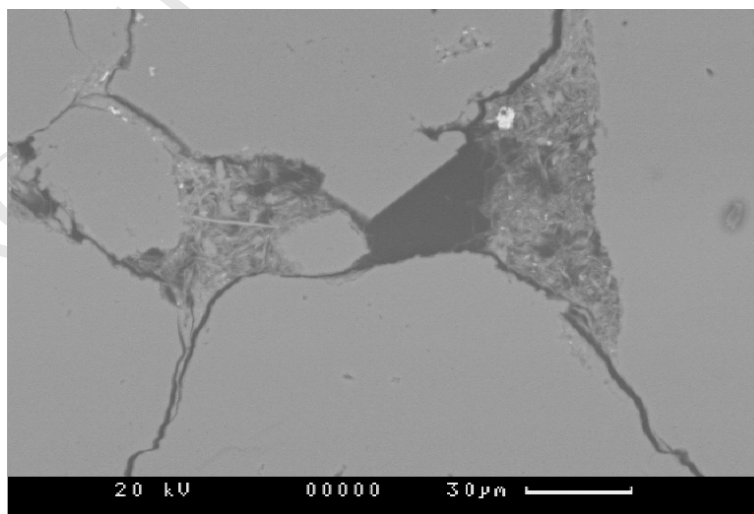


Figure 22 BSEM micrograph showing dilated grain boundaries, which offer preferential pathways for fluid flow at low confining pressures.

4.3 Clay content vs fault permeability relationships

Most fault seal analysis workflows populate simulation models with fault transmissibility multipliers that are based on a link between clay content and fault permeability (for recent reviews, see Jolley et al., 2007; Yielding et al., 2010; Manzocchi et al., 2010). The results collected during the current study (e.g. **Figure 20**) are consistent with several other studies that show a generally poor correlation between clay content and fault permeability (e.g. Fisher and Knipe, 1998; 2001; Sperrevik et al., 2002; Jolley et al., 2007; Frischbutter et al., 2017). The relationship between clay content of the protolith and fault rock type is also not obvious as that suggested by Fisher and Knipe (1998, 2001).

It could be argued that much of the scatter in **Figure 20** is increased dramatically by the inclusion of fault rock samples from the Triassic of the northern North Sea. There are some grounds as to why this dataset should be excluded. In particular, the clay content obtained by QXRD appears far greater than observed by BSEM analysis. This reflects the presence of large quantities of coarse-grained detrital chlorite in these samples, which cannot be easily distinguished from finer grained authigenic chlorite from the QXRD results. Also, there is some evidence that faulting was associated with injection of sand, which would mean that the clay content of the fault would not be directly related to the composition of the adjacent sandstone. Discounting these outliers creates an exponential relationship between clay content and brine permeability (**Figure 23**) following the relationship:

$$k_b(5000 \text{ psi}) = 25e^{-0.6C} \quad (5)$$

where k_b (5000 psi) is the brine permeability at 5000 psi net stress (mD) and C is the clay content (%). It should be noted that although **Figure 23** shows a broad relationship between brine permeability and clay content it shows that no such relationship exists when only phyllosilicate-framework fault rocks are considered, which is consistent with previous studies (e.g. Fisher and Knipe, 2001).

There are also theoretical grounds to suspect that there should indeed be a large amount of scatter on plots of permeability vs. clay content and that there should not in fact been firm boundaries between the type of fault rock that develops and the clay content of the protolith. In particular, porosity and permeability of sand-clay mixtures are controlled by many other factors than simply clay content. For example, Revil and Cathles (1999) as well as Revil et al. (2002) showed that the permeability of sand-clay mixtures (i.e. fault gouge) is controlled by the porosity and permeability of the clay matrix, the critical porosity of the sand (i.e. porosity when there is no clay present) as well as the permeability of the sand and the critical porosity. The critical porosity of the sand is controlled by grain sorting and its permeability is controlled by both grain-sorting and grain-size. Accounting for these factors may explain much of the scatter on plots of clay content vs. fault rock permeability.

Revil and Cathles (1999) presented the following model for the permeability of clay-sandstone mixtures, k_m ,

$$k_m = k_{sd}^{1-\frac{V_{cl}}{\phi_{sd}}} \times k_{cfs}^{V_{cl}/\phi_{sd}}, \quad 0 \leq V_{cl} \leq \phi_{sd} \quad (6a)$$

$$k_m = k_{sh} V_{cl}^{3/2}, \quad \phi_{sd} \leq V_{cl} \leq 1 \quad (6b)$$

where ϕ_{sd} and k_{sd} are the porosity and permeability of the clay-free sand, k_{sh} is the permeability of the shale end-member and:

$$k_{cfs} = k_{sh} \phi_{sd}^{3/2} \quad (7)$$

To assess the implications of this model for fault rock permeability data on the impact of grain-sorting on porosity and grain-size and sorting on permeability have been incorporated into the model of Revil and Cathles (1999). **Figure 24** shows the impact of two sand clay mixtures on clay-permeability relationships; both assume the shale end-member has a permeability of 10 nD. The first sand is assumed to be coarse grained and well sorted with a porosity of 43.1% and a permeability of 5 D. The second sand is assumed to be fine-grained, very poorly sorted with a porosity of 29% and permeability of 50 mD. The results show that for a given clay content the mixtures can have up to two orders or magnitude difference in permeability. These differences can be further extenuated by incorporating the impact of different burial histories and different end-member shale permeabilities.

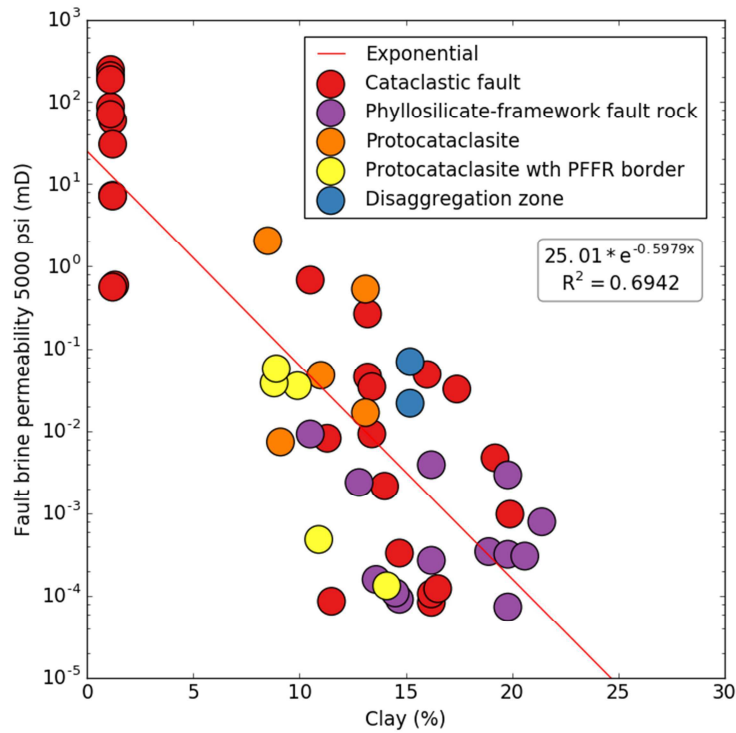


Figure 23 Plot of clay content vs brine permeability for the samples analysed during this study; with the faults from Triassic sandstones excluded. The red line represents the exponential regression.

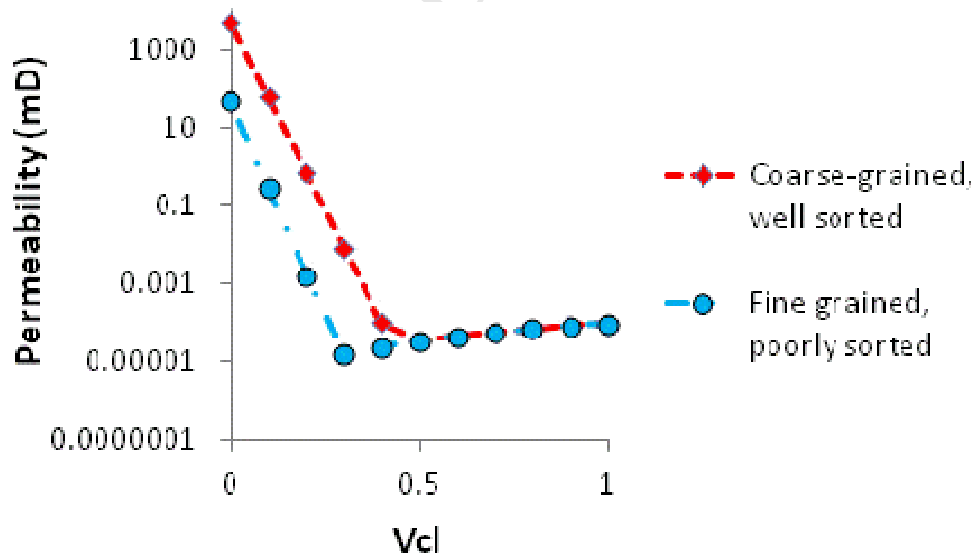


Figure 24 Plot of permeability of a sand-clay mixture as a function of clay content where the initial sands have different grain-sizes and grain-sorting, hence porosity and permeability (see text for details).

4.4 CT scans as a screening tool for fault rock studies

It is common practice to conduct fault seal analysis studies during the appraisal of petroleum reservoirs in which the microstructural and petrophysical properties of a full range of fault rocks present in core are analyzed (e.g. Knai and Knipe, 1998; Ellevset et al., 1998; Porter et al., 2000, 2005). However, it's probably only worth obtaining such detail measurements on fault rocks that are likely to impact fluid flow. Several studies indicate that a permeability contrast (i.e. reservoir/fault permeability) of at least 10,000 is required for faults to significantly impact fluid flow (Walsh et al., 1998; Yaxley, 1987). The results from the current study indicate that such fault rocks have a large contrast in CT numbers with their host sediment. It therefore seems possible that CT scans can be used as a rapid and cheap method for identifying fault rock samples that are worth sampling for fault seal analysis studies. Such screening could significantly reduce the number of samples that are analyzed and thus reduce the costs of fault seal analysis studies where juxtaposition analysis indicates that faults juxtaposing reservoir against reservoir are present.

5 Conclusions

Industry has collected a large amount of data on the permeability of fault rocks found in siliciclastic petroleum reservoirs. Unfortunately, much of these data were collected using inappropriate laboratory protocols: low confining pressures and distilled water as the permeant. New laboratory measurements conducted at high confining pressures and with formation compatible brine indicate that making measurements using distilled water almost compensates for the impact of making the measurements at low stress. These results indicate that legacy fault rock permeability data may still be useful where state-of-the-art data are not available.

However, it is recommended that where possible fault rock permeability measurements are made at in situ stress conditions using formation compatible brine.

The permeability of fault rock samples analysed in the laboratory is very stress dependent but this is unlikely to be the case in the subsurface for reservoirs buried to depths beyond where mechanical compaction has ceased so long as stresses do not result in fault reactivation. This result significantly simplifies fault seal analyses for many reservoirs because it means that no account needs to be taken of stress dependent fault permeability unless there is a chance that fault reactivation is likely to occur.

Clay – fault rock permeability relationships are likely to be intrinsically scattered in large datasets due to differences in the grain-size and sorting of the sand end-member as well as differences in permeability of the clay end-member. This also means that it is not possible to provide definitive clay values that separate different fault rock types. Overall, it is recommended that clay-fault permeability relationships are established for each reservoir undergoing fault seal analysis.

Industry is not likely to obtain significant value analysing the permeability of fault rocks that do not impact flow. It is therefore recommended that CT-scanning is used as a tool to identify the samples that are most likely going to produce relevant results for use in fault seal analyses.

Acknowledgements

We would like to thank BHP, ConocoPhillips, Shell, Statoil, and Wintershall for funding this research as well as NED for funding the studentship of Dr Javed Haneef.

References

- Al-Busafi, B., Fisher, Q.J. and Harris, S.D. (2005) The importance of incorporating the multiphase flow properties of fault rocks into production simulation models. *Marine and Petroleum Geology*, **22**, 365-374.
- Al-Hinai, S., Fisher, Q.J., Al-Busafi, B., Guise, P. and Grattoni, C.A. (2008) Relative Permeability of Faults: An Important Consideration for Production Simulation Modelling. *Marine and Petroleum Geology*, **25**, 473-485.
- Amaefule, J.O., Wolfe, K., Walls, J.D., Ajufo, A.O. and Peterson, E. (1986) Laboratory Determination of Effective Liquid Permeability in Low-Quality Reservoir Rocks by the Pulse Decay Technique. Paper SPE-15149-MS, Society of Petroleum Engineers. Paper prepared for presentation at the 56th California Regional Meeting of the Society of Petroleum Engineers, Oakland, CA, April 2-4, 1986.
- Brace, W.F., Walsh, J.B. and Frangos, W.T. (1968) Permeability of Granite under High Pressure. *Journal of Geophysical Research*, **73**, No. 6, pp. 2225- 2236.
- Byrnes, A.P. and Castle, J.W. (2000) Comparison of Core Petrophysical Properties Between Low-Permeability Sandstone Reservoirs: Eastern U.S. Medina Group and Western U.S. Mesaverde Group and Frontier Formation. Paper SPE-60304-MS, Society of Petroleum Engineers. Paper prepared for presentation at

- the 2000 SPE Rocky Mountain Regional/Low Permeability Reservoirs Symposium and Exhibition, Denver, Colorado, 12–15 March 2000.
- Calhoun, Jr., J. C., Lewis, Jr., M., and Newman, R.C. (1949) Experiments on the Capillary Properties of Porous Solids. *Trans AIME* **186**, 189–196.
- Collins, R.E. (1976) *Flow of Fluids through Porous Materials*. The Petroleum Publishing Co., Tulsa, OK.
- Donaldson, E.C. and Tiab, D. (2004). *Theory and Practice of Measuring Reservoir Rock and Fluid Transport Properties*. Gulf Professional Publishing, Elsevier.
- Ellevset, S. O., Knipe, R. J., Olsen, T. S., Fisher, Q. J. and Jones, G. (1998) Fault rock properties prediction in the Sleipner Vest Field, Norwegian Continental Shelf: a method of providing detailed quantitative input for reservoir simulation and well planning. In: G. Jones, Q.J. Fisher and R. J. Knipe, (Eds.), *Faulting and Fault Sealing in Hydrocarbon Reservoirs*. Geological Society, London, Special Publication, **147**, 283-298.
- Eardley., N. (2017) *Improved Reservoir Characterisation and Appraisal of Tight Gas Sandstones*. PhD thesis. University of Leeds.
- Fisher, Q. J. and Knipe, R. J. (1998) Fault sealing processes in siliciclastic sediments. In: Jones, G., Fisher, Q.J. & Knipe, R.J. (eds) *Faulting, Fault Sealing and Fluid Flow in Hydrocarbon Reservoirs*. Geological Society, London, Special Publications, **147**, 117–134.
- Fisher, Q.J. and Knipe, R.J. (2001) The permeability of faults within siliciclastic petroleum reservoirs of the North Sea and Norwegian Continental Shelf. *Marine and Petroleum Geology*, **18**, 1063–1081.

- Fisher, Q.J. and Jolley, S.J. (2007) Treatment of faults in production simulation models. *In: Jolley, S. J., Barr, D., Walsh, J. J. & Knipe, R. J. (eds) Structurally Complex Reservoirs*. Geological Society, London, Special Publications, **292**, 219-233.
- Frischbutter, A.A., Fisher Q.J., Namazova, G. and Dufour S. (2017) The value of fault analysis for field development planning. *Petroleum Geoscience*, 23, pp. 120-133. doi: 10.1144/petgeo2016-053.
- Hillier, S. (1999) Use of an air brush to spray dry samples for X-ray powder diffraction. *Clay Minerals*, **34**, 127–135.
- Hillier, S. (2000) Accurate quantitative analysis of clay and other minerals in sandstones by XRD: comparison of a Rietveld and a reference intensity ratio (RIR) method and the importance of sample preparation. *Clay Minerals*, **35**, 291–302.
- Jolley, S.J., Dijk, H., Lamens, J.H., Fisher, Q.J., Manzocchi, T., Eikmans, H. and Huang, Y. (2007) Faulting and fault sealing in production simulation models: Brent Province, northern North Sea. *Petroleum Geoscience*, **13**, 321–340.
- Jones, S. (1997) A technique for faster pulse-decay permeability measurements in tight rocks. *SPE Formation Evaluation*, 19-25.
- Kilmer, N. H., Morrow, N. R. and Pitman, J. K. (1987) Pressure sensitivity of low permeability sandstones. *J. Petr. Sci. and Eng.* **1**, 65-81.
- Knai, T.A. and Knipe., R.J. (1998) The impact of faults on fluid flow in the Heidrun Field, *In: Jones, G.; Fisher, Q.J.; Knipe, R.J. (Ed) Faulting and fault sealing and fluid flow in hydrocarbon reservoirs*, Geological Society Special Publication, **147**, Geological Society of London, 269-282.

- Lever, A. and Dawe, R.A. 1987. Clay migration and entrapment in synthetic porous media. *Marine and Petroleum Geology* **4**(2):112-118. DOI: 10.1016/0264-8172(87)90027-4
- Manzocchi, T., Heath, A.E., Walsh J.J. & Childs, C. (2002) The representation of two-phase fault-rock properties in flow simulation models. *Petroleum Geoscience*, **8**, 119–132.
- Manzocchi, T., Walsh, J.J., Nell, P. & Yielding, G. (1999) Fault transmissibility multipliers for flow simulation models. *Petroleum Geoscience*, **5**, 53–63.
- Manzocchi, T., Childs, C. and Walsh, J.J. (2010) Faults and fault properties in hydrocarbon flow models. *Geofluids*, **10**, 94–113. doi: 10.1111/j.1468-8123.2010.00283.x
- Melrose, J.C. (1990) Valid capillary pressure data at low wetting phase saturation. Paper SPE 18331. SPE Reservoir Engineering. 95-99.
- Morrow, C.A., Shi, L.Q., Byerlee, J.D. (1984) Permeability of fault gouge under confining pressure and shear stress. *J Geophys. Res.*, **89**, 3193–3200.
- Olson, R.E. and Daniel, D.E. (1981) Measurement of the Hydraulic Conductivity of Fine-Grained Soils. In Zimmie, T.F., and Riggs, CO. (Eds.), *Permeability and Groundwater Contaminant Transport*. ASTM Spec. Tech. Publ., **746**, 18-64.
- Olson, M. S., Tillman, F. D. J., Choi, J. W. and Smith, J. A. 2001. Comparison of three techniques to measure unsaturated zone air permeability at Picatinny Arsenal, NJ. *J. Contam. Hydrol.* **53**: 1–19.
- Porter, J.R., McAllister, E., Fisher, Q.J., Knipe, R.J., Condliffe, D.M., Kay, M.A. Stryliandes, G. and Sinclair, I.K. (2005) Impact of fault damage zones on reservoir performance in the Hibernia Oilfield (Jeanne d'Arc Basin,

- Newfoundland): an analysis of structural, petrophysical and dynamic well test data. In: Hiscott, R. & Pulham, A. (eds) *Petroleum Resources and Reservoirs of the Grand Banks, Eastern Canadian Margin*, Geological Association of Canada Special Paper, **43**, 129-142.
- Porter, J.R., Knipe, R.J., Fisher, Q.J., Farmer, A.B., Allin, N.S., Jones, L.S. and Palfrey, A.J., Garrett, S.W. and Lewis, G. (2000) Deformation processes and down-slope movement in the Britannia Field, UKCS. *Petroleum Geoscience*, **6**, 241-254.
- Revil, A. and Cathles, L. M. (1999) Permeability of shaly sands. *Water Resources Research*, **35**, 651–662.
- Revil, A., Grauls, D., and Brevart, O. (2002) Mechanical compaction of sand/clay mixtures. *J. Geoph. Res.*, **107** (B11), pp. ECV 11-1- ECV 11-15.
- Segura, J.M., Fisher, Q.J. Crook, A.J.L. Angus, D.A, Kendall, J.M. and Dutko, M. (2011) Reservoir Stress Path Characterization and its Implications for Fluid-Flow Production Simulations. *Petroleum Geoscience*, **17**, 335-344.
- Saillet, E. and Wibberley, C.A.J. (2013) Permeability and flow impact of faults and deformation bands in high-porosity sand reservoirs: Southeast Basin, France, analog. *American Association of Petroleum Geologists*, 97,437-464.
- Sibson, R.H. (1977) Fault rocks and fault mechanisms. *J. Geol. Soc. London*, **133**, 191-213.
- Sperrevik S., Gillespie, P.A., Fisher, Q.J., Halvorsen, T. and Knipe, R.J. (2002) Empirical Estimation of Fault Rock Properties In: Koestler, A.G. & Hunsdale, R. (eds) *Hydrocarbon Seal Quantification*. Norwegian Petroleum Society (NPF) Special Publication, Amsterdam, **11**, 109–125.

- Thomas, R.D. and Ward, D.C. (1972) Effect of overburden pressure and water saturation on gas permeability of tight sandstone cores. Paper SPE-3634-PA, Society of Petroleum Engineers. *Journal of Petroleum Technology*, **24**, 120-124.
- Tueckmantel C., Fisher Q.J., Grattoni C.A. and Aplin A.C. (2012) Single- and two-phase fluid flow properties of cataclastic fault rocks in porous sandstone, *Marine and Petroleum Geology*, **29**, 129-142.
- Walsh, J.J., Watterson, J., Heath, A.E. and Childs, C. (1998) Representation and scaling of faults in fluid flow models. *Petroleum Geoscience*, **4**, 241-252.
- Wei, K. K., Morrow, N. R. and Brewer, K. R. (1986) Effect of fluid, confining pressure, and temperature on absolute permeabilities of low permeability sandstones. Paper SPE-13093-PA, Society of Petroleum Engineers. *SPE Formation Evaluation* **14** (4), 413 – 423.
- Yaxley, L.M. (1987) Effect of a partially communicating fault on transient pressure behavior. *SPE Formation Evaluation*, **2**, 590-598.
- Wibberley, C.A.J. and Shimanoto, T. (2003) Internal structure and permeability of major strike-slip fault zones: the Median Tectonic Line in Mie Prefecture, Southwest Japan. *Journal of Structural Geology*, **25**, 59-78.
- Yaxley, L.M., (1987) Effect of a partially communicating fault on transient pressure behaviour. *SPE Formation Evaluation*, **2**, 590-598.
- Zijlstra, E.B., Reemst, P.H.M. and Fisher., Q.J. (2007) Incorporation of fault properties into production simulation models of Permian reservoirs from the southern North Sea. Geological Society, London, Special Publications, **292**, 295-308. doi: 10.1144/SP292.17

- Fault rocks permeabilities measured at in situ stresses with formation brines.
- Fault permeability is sensitive to stress and brine composition.
- Legacy data collected at low stress with low salinity brine is still useful.
- A poor correlation exists between clay content and fault permeability.
- CT scanning is a valuable tool to select faults for permeability analysis.
- Fault permeability is not stress sensitive in reservoirs unless close to failure